Processing and Application of Ceramics 15 [1] (2021) 87–94
https://doi.org/10.2298/PAC2101087H

Structure and optical properties of porous SiC film grown by magnetron sputtering on porous anodic aluminium oxide template

Zhenhua He*, Jieling Li, Canhui Liu*, Shifei Zhu

School of Information Engineering, Wuhan University of Technology, Wuhan 430070, PR China

Received 29 June 2020; Received in revised form 11 December 2020; Accepted 26 February 2021

Abstract

Porous fluorescent SiC films were deposited by magnetron sputtering (MS) using porous anodic aluminium oxide (AAO) template. In the first step AAO was carefully placed on the Si substrate and then coated with SiC film using magnetron sputtering at the deposition temperature of 873 K for different times. The pore diameter, pore spacing and thickness of the double pass porous AAO template were 300, 450 and 500 nm, respectively. The SiC film deposited for 60 min showed macroporous structure with the pore size of 200 to 250 nm and pore spacing of 450 nm. The photoluminescence (PL) spectrum of the porous SiC film ranged from 400 to 700 nm. The band gap of SiC is 2.305 eV, and the phonon energy of phonon participating in PL of SiC is estimated at 0.075 eV. The source of phonon participating in PL of SiC may be from phonon scattering of silica/SiC interface in porous SiC film. The porous AAO template assisted magnetron sputtering is a promising technical processing for the fabrication of macroporous fluorescent SiC film.

Keywords: *porous SiC film, anodic aluminum oxide substrate, magnetron sputtering, photoluminescence*

I. Introduction

Silicon carbide (SiC) is one of the most potential materials for the third generation semiconductors. SiC has plenty of excellent properties, such as wide band gap, high critical breakdown electric field, high thermal conductivity, high oxidation resistance, high chemical stability, high carrier saturation drift rate and high radiation resistance [1–5]. Therefore, SiC can be applied in high temperature, high frequency, radiation resistance and high power devices [2]. Furthermore, because of its unique band gap (2.3–3.3 eV) [6], SiC can also be used in blue, green or ultraviolet light emitting devices and photoelectric sensor detectors [7]. However, the semiconductor band gap of bulk SiC is indirect, the photoluminescence (PL) of SiC needs the participation of phonons with the appropriate momentum to satisfy the conservation of momentum. Consequently, bulk SiC has poor PL properties, which limits the optical applications of SiC.

Porous structure was proved to be effective for improving PL property of SiC [8–10]. Matsumoto *et al.* fabricated porous n-type 6H-SiC by electrochemical anodization method using HF-ethanol solution [8]. Blue shift and enhanced luminescence of porous 6H-SiC were observed in the luminescence spectrum of porous 6H-SiC and bulk 6H-SiC [8]. The luminescence peak of porous 6H-SiC and bulk 6H-SiC were 460 nm (2.70 eV) and 590 nm (2.10 eV), respectively [8]. Petro-Koch *et al.* [9] studied room temperature and low temperature bulk and porous 6H-SiC luminescence by using electrochemical etching method. In the luminescence spectrum of the bulk and porous 6H-SiC, the luminescence peaks were both located at 2.65 eV with the excitation energy of 3.5 eV [9]. The enhanced luminescence of porous 6H-SiC compared to bulk 6H-SiC were observed at both 5 K and 300 K temperature [9]. Lu *et al.* [10,11] prepared N-B co-doped 6H-SiC with 10 μm porous surface structure by anodic oxidation method. After passivation with 20 nm thick Al_2O_3, the PL intensity from the porous layer was significantly enhanced by a factor of more than 1225 [10,11]. Fluorescent SiC with porous surface can be used for high performance and rare-earth element free white light emitting applications [10,11]. Li *et al.* [12,13] used two-dimensional (2D) porous structure to improve PL property of SiC.

In this paper, we propose a new method, which combines porous anodic aluminium oxide (AAO) template

*Corresponding authors: tel: +86 87651800,
e-mail: *zhenhuahe@whut.edu.cn* (Zhenhua He),
xy1801lch@whut.edu.cn (Canhui Liu)

and magnetron sputtering, to fabricate porous SiC film. Magnetron sputtering technique has the advantages of high speed, low temperature, low cost and strong adhesion of coating, which have a significant impact in application areas including hard, wear-resistant coatings, low friction coatings, corrosion-resistant coatings, decorative coatings and coatings with specific optical, or electrical properties [14]. We propose forward SiC 2D porous structure as shown in Fig. 1 by using AAO template to improve PL property of SiC. In the designed structure, SiC was deposited on porous AAO/Si(100) substrate. The microstructure, Raman spectrum, room-temperature PL spectrum, low-temperature PL spectrum, Ultraviolet-Visible spectrum and PL mechanism of porous SiC film by porous AAO template assisted magnetron sputtering processing were investigated. By peak splitting simulation of the fine structure of PL spectrum of SiC, the energy of phonon participation in PL of SiC was estimated.

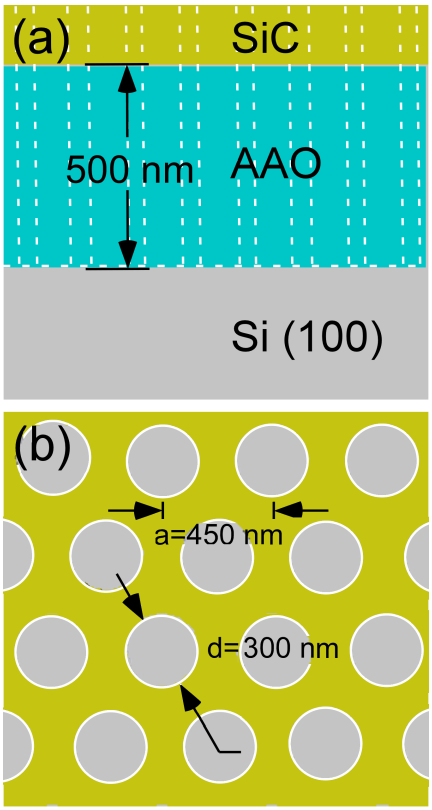

Figure 1. Diagrams of the designed porous SiC film structure: a) front-view and b) top-view images

II. Experimental

The proposed films had three-layer structure: i) the Si(100) single crystal substrate as the bottom layer, ii) the double pass porous AAO film (pore diameter 300 nm, pore spacing 450 nm, thickness 500 nm, Top-membranes Technology Co. Ltd.) as the template middle layer and iii) the SiC film designed as the upper layer. Because of the AAO film brittleness, the company (Topmembranes Technology Co. Ltd.) coated a layer of polymethacrylic acid (PMAA) on the AAO template surface to make transfer of the AAO film to the target substrate easier. The PMAA/AAO films were cut to a suitable size and carefully placed on the Si substrate with tweezers. The transfer process of the AAO templates was prone to failure and the process required several attempts. Finally, the PMAA/AAO/Si heterostructure was immersed in an acetone solution to dissolve PMAA and the SiC film was coated on AAO/Si(100) template by magnetron sputtering (MS). The target for MS was bulk SiC (purity 99.9%, α-SiC). The deposition process was performed with radio frequency (RF) power of 140 W under Ar pressure of 5 Pa and Ar gas flow of 40 sccm. SiC films were deposited at 873 K for 1, 5, 10, 15, 30 and 60 min and the samples denoted SiC-1, SiC-5, SiC-10, SiC-15, SiC-30 and SiC-60, respectively, were obtained.

The microstructure of the porous SiC films was observed using high resolution field emission electron microscope (JSM-7500F, JEOL) and transmission electron microscopy (TEM, F200S, TALOS, Czech Republic). The TEM samples were prepared by FIB equipment (FIB, NanoLab G3 UC, HELIOS, U.S.A). The Raman spectra were tested by LabRAM HR Evolution using 1% filter for 5 s excited by 532 nm laser. The room tem-

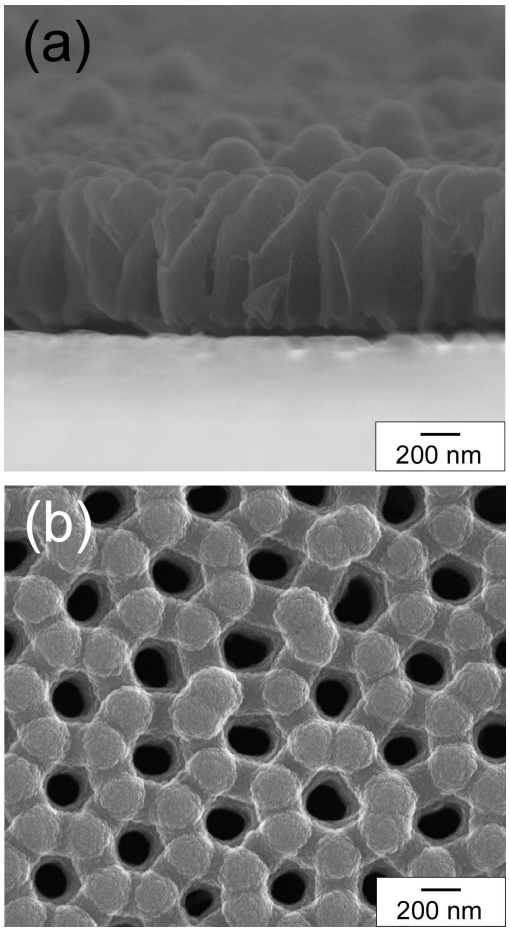

Figure 2. Microstructure of the prepared porous SiC film with deposition time of 60 min: a) cross section and b) surface images

perature PL spectra were measured using 325 nm laser with power of 7.5 mW. Low temperature fluorescence spectra were performed using vacuum sample chamber at temperature of 83 K. The ultraviolet-visible spectrum of absorbance and reflectance was tested by UV-VIS-NIR spectrometer (Lambda 750S, PerkinElmer) with wavelength ranging from 200 to 800 nm.

III. Results and discussion

The SiC film deposited for 60 min (SiC-60) has a 'honeycomb' structure composed of closely arranged 'hexagons', with periodicity (Fig. 2), and each hexagon point has a 'mushroom cloud' like protrusion structure. Combining the vertical-section and the top view of the sample, it can be seen that the SiC film is a three-dimensional structure, and the SiC tends to adhere to the 'hexagon' vertexes during sputtering. The SiC film deposited for 60 min (Fig. 2) shows macroporous structure with the pore size of 200 to 250 nm and pore spacing of 450 nm. The thickness of SiC film is about 230 to 530 nm with the average thickness of 272 nm. Because of the amorphous phase of the porous AAO template, the SiC film deposited on AAO template at 873 K should be a periodically amorphous phase semiconductor.

Figure 3 shows surface microstructure of the porous SiC films deposited for different times ranging from 1 to 30 min. The inner surface of porous AAO was coated by SiC films with increasing deposition time. The SiC-10 film deposited for 10 min started to grow also on the edge positions of the surface hole, showing periodic hexagon structure. From 10 to 30 min deposition time, the width of the SiC in periodic hexagon structure increased from 60 to 120 nm. The cross section microstructures of the porous SiC films deposited for different times are shown in Fig. 4. Because of the amor-

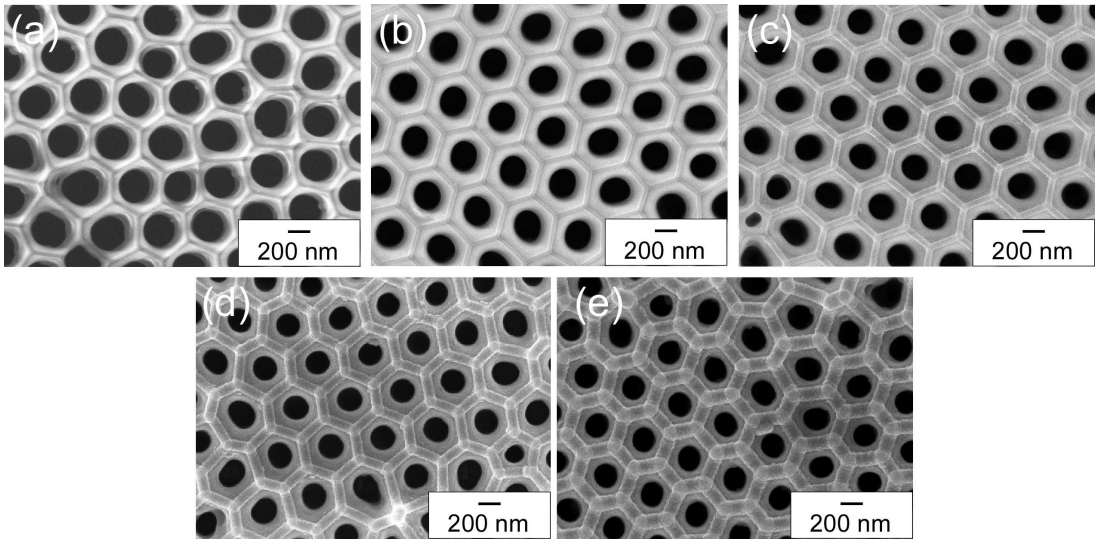

Figure 3. Surface microstructure of porous SiC films deposited for different times: a) 1 min (SiC-1), b) 5 min (SiC-5), c) 10 min (SiC-10), d) 15 min (SiC-15) and e) 30 min (SiC-30)

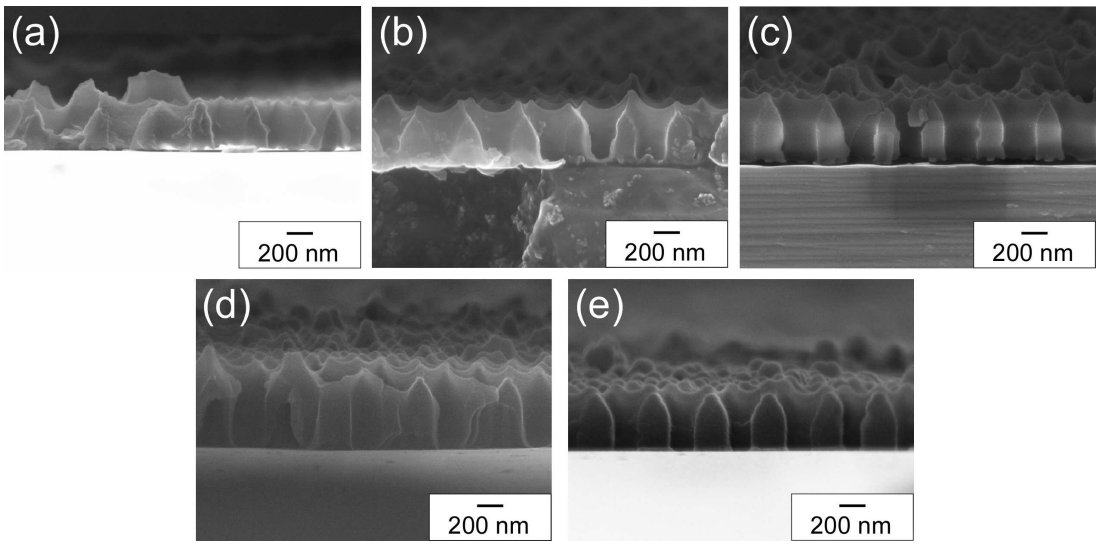

Figure 4. Cross section microstructure of porous SiC films deposited for different times: a) 1 min (SiC-1), b) 5 min (SiC-5), c) 10 min (SiC-10), d) 15 min (SiC-15) and e) 30 min (SiC-30)

phous characteristic of SiC and alumina, it is hard to distinguish SiC from alumina middle layer in SEM figures. Pore structure of the SiC films in the middle position and bottom position shows cylindrical hole shape, while in the upper position shows inverted cone shape. According to the results presented in Figs. 2, 3 and 4, it can be concluded that the pore diameter of porous film decreased from about 300 to 200–250 nm with increasing deposition time from 1 to 60 min. With increasing deposition time from 10 to 60 min, the width of top surface SiC film in periodic hexagon structure increased from 60 nm to about 200 nm.

TEM microstructure, selected area electron diffraction (SAED) and element surface scanning images of the SiC film deposited for 60 min were shown in Fig. 5. The sample for TEM was coated by ultrathin amorphous carbon film (thickness below 5 nm, using spark discharge technique) and then prepared by FIB technique. In FIB processing, the sample surface was coated with Pt films to protect the SiC film and transfer the cut TEM sample out of the FIB equipment. From the crystalline interplanar spacing of 0.276 nm (Fig. 5b) the corresponding crystal face group was identified as Si (200). The Si (100) substrate was identified by Fig. 5b. From the diffuse central spot characteristic of the SiC film SAED data in Fig. 5c, the amorphous phase of SiC film was identified. Through Figs. 5d,e,f we can distinguish SiC film from alumina middle layer clearly. The amorphous SiC was coated on the surface of alumina middle layer. The top surface of the SiC film and alumina middle layer in cross section showed round shapes and sharp-pointed shapes, respectively. After the SiC deposition process, the surface area of porous film increased.

From Raman spectra presented in Fig. 6, the peaks of the SiC films without AAO template appeared at 940 cm^{-1} to 981 cm^{-1} containing 972 cm^{-1} (3C-SiC) and 965 cm^{-1} (6H-SiC) peaks [15]. It can be concluded that the SiC films with AAO template are amorphous SiC. Because of the upward trend of the curve of SiC films with AAO, the PL of the porous SiC films can be excited by 532 nm laser.

It can be seen from Fig. 7 that the SiC samples deposited for 1 to 60 min reached their peaks at 441 nm, which were the emission peaks caused by the oxygen vacancy defects of silica in the sample [8,16]. In addition, the peak centres of the SiC-1 (sputtered for 1 min), SiC-5 (sputtered for 5 min) and SiC-10 (sputtered for 10 min) samples are at 520 nm, and the peak intensity decreases with the increasing of deposition time. It shows that the samples SiC-1, SiC-5 and SiC-10 have the same luminescent mechanism and the luminescent property decreases with increasing SiC deposition time. The above PL mechanism of the samples SiC-1, SiC-5 and SiC-10 at the peak of 520 nm may be due to surface defects (such as oxygen defects) on the surface of porous AAO middle layer [17]. For the samples SiC-1, SiC-5 and SiC-10, with increasing deposition time from 1 min to 10 min, the surface defects of the porous AAO middle layer were filled by SiC film, and the number of surface defects in the middle layer decreased. So the intensity of 520 nm peak decreased with the increase of deposition time from 1 to 10 min.

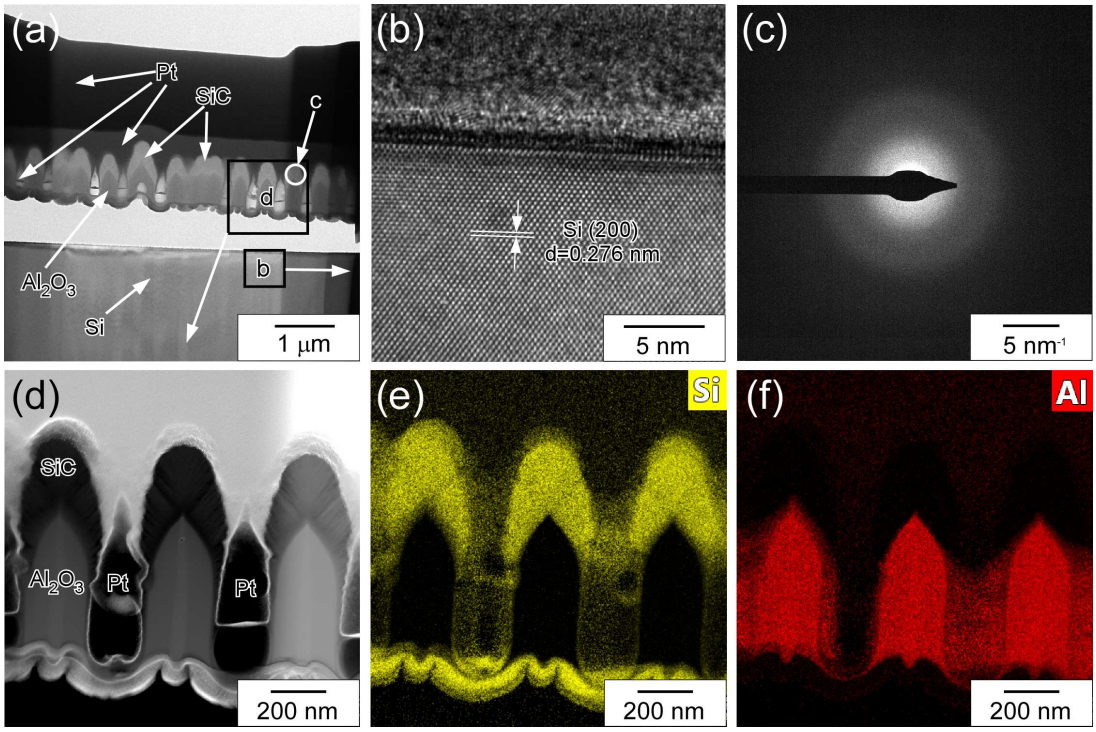

Figure 5. TEM microstructure of porous SiC film deposited for 60 min. High resolution TEM image of the selected area (b), selected area electron diffraction (SAED) pattern of the selected area (c), high resolution SEM image of the selected area (d) and corresponding Si (e) and Al (f) element surface scanning images

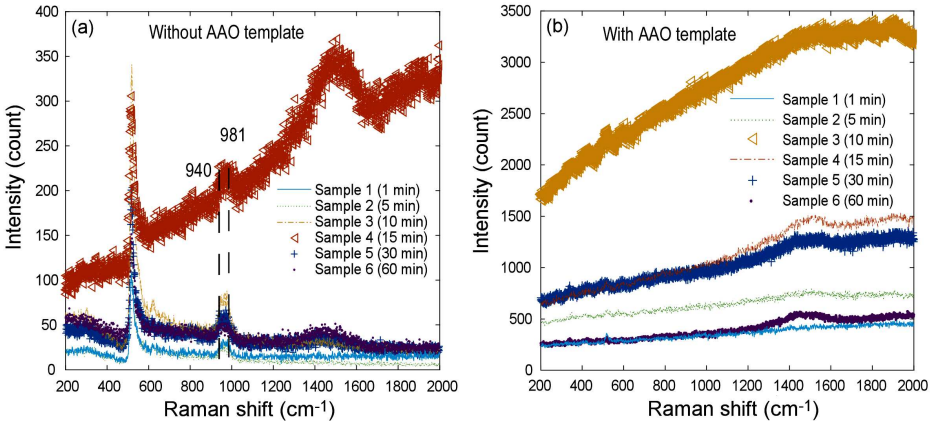

Figure 6. Raman spectra of the SiC films deposited for different times at the section: a) without AAO template and b) with AAO template

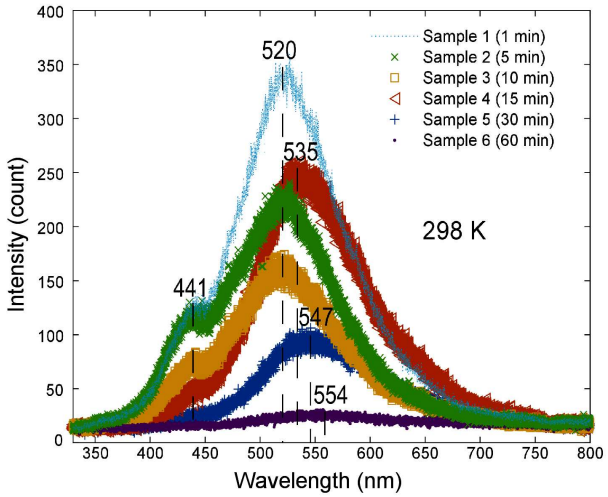

Figure 7. The room temperature PL spectra of porous films deposited for different times from 1 to 60 min

Figure 7 also shows that the peak value centre for the samples SiC-15, SiC-30 and SiC-60 moves to 535, 547 and 554 nm, respectively. It can be seen that the peak centres of SiC films have red shift with increasing sputtering time from 15 to 60 min and the peak intensity decreases with increasing sputtering time. This shows that when the sputtering time is more than 10 min, the main luminescence mechanism of the porous SiC films change from surface defects PL of porous AAO middle layer to SiC PL. With increasing the sputtering time from 15 to 60 min, the main luminescence mechanism of porous SiC films changed from quantum confinement effect of SiC film to intrinsic PL of SiC film. The longer the sputtering time, the more obvious the red shift phenomenon of PL spectrum and the lower the peak value. It can be concluded that the main luminescence mechanism of the porous SiC-60 film is intrinsic PL of SiC film.

In this experiment, the sample SiC-60 with the longest sputtering time and the intrinsic luminous effect of SiC is taken for photoluminescence experiment under the condition of 83 K, as shown in Figs. 8 and 9. From Fig. 9, it can be roughly seen that the PL spectrum of the sample SiC-60 has five peaks based on the Gauss simulation. There are two peaks at around 2.3 eV. Therefore, it can be inferred that the sample SiC-60 produces PL at 83 K.

The simulation data of each wave peak is shown in Table 1. Five peaks (peak 1 to peak 5), numbered from left to right shown in Fig. 9, are simulated according to PL spectrum of the sample SiC-60 at 83 K. The ratio of PL peak 2.88 eV (peak 2) is 13.98%. The ratios of PL peaks of 2.38 eV (peak 3) and 2.23 eV (peak 4) are 73.52%, which is more than ⅔ of the total peak area, which indicates that the PL of the sample SiC-60 is mainly caused by the generation of peaks of 2.38 and 2.23 eV. It can be seen that the waveforms of peaks of 2.38 and 2.23 eV are highly symmetrical. According to the PL mechanism of indirect band gap semiconductor, those are the PL peaks of SiC, that is, SiC absorbs or releases one phonon to carry on PL. From that, we can calculate the phonon energy of phonon participation in PL of SiC, E_{ph}, and the band gap width of SiC, E_g. The E_{ph} and E_g of SiC were 0.075 and 2.305 eV, respectively.

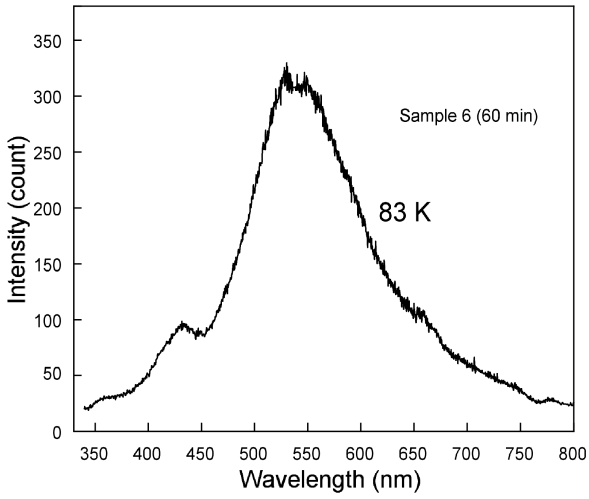

Figure 8. Low temperature PL spectrum of porous SiC film of the sample SiC-60 at 83 K

Table 1. Data of PL peak splitting simulation of the sample SiC-60 at 83 K

Peaks number	FWHM [eV]	Maximum intensity [Counts]	Peak average center [eV]	Percentage of peak area of fitting data [%]
1	0.40	12	3.34	2.50
2	0.39	67	2.88	13.98
3	0.43	161	2.38	36.76
4	0.43	161	2.23	36.76
5	0.39	48	1.91	10.00

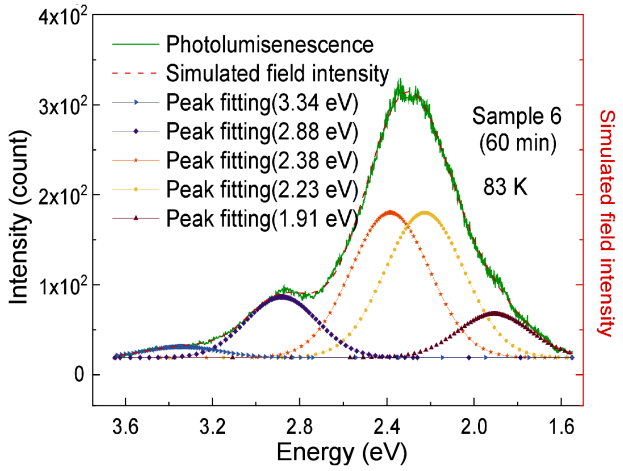

Figure 9. The low temperature PL and simulated PL spectra of porous SiC film deposited for 60 min at testing temperature of 83 K

The peak of 3.34 eV may belong to the band gap of 6H-SiC. The peak centre of peak 2 is at 2.88 eV, which is the emission peak caused by the oxygen vacancy defects of silica in SiC film. The centre of peak 5 is at 1.91 eV. The corresponding wavelength is 649 nm. The wavelength of the 1.91 eV peak is twice the wavelength of the PL laser (325 nm). The peak 5 of 1.91 eV may be caused by the 325 nm laser used in the experiment.

At low temperature of 83 K, the phonon of E_{ph} (0.075 eV) cannot be produced by SiC. Photon energy difference of 325 nm laser (3.82 eV) and peak 2 of 2.88 eV is 0.94 eV, which is the 12.5 times of E_{ph} (0.075 eV). The energy exchange between photons and phonons is quantized. According to the energy level formula of one dimensional identical harmonic oscillator of phonon:

$$E = (N + 1/2)E_{ph} \quad (1)$$

the N is calculated at 12. One PL process of peak 2 can produce up to 12 phonons. The source of phonon participating in PL of SiC may be from PL of oxygen defect of silica in the SiC film. Based on the ratio of PL peak area of oxygen defect of Silica and SiC film, the photon transformation ratio of PL peak 2 is 43.82%.

Figure 10 shows the ultraviolet-visible (UV) spectrum of the porous SiC film deposited for 60 min. From UV absorbance spectrum, there are six absorbance peaks at 223, 262, 318, 406, 480 and 528 nm. From reflectance spectrum, the reflectivity reached more than 55% with wavelength ranging from 400 to 800 nm. The special UV spectrum properties of the SiC film may be caused by the porous structure and high surface area.

The schematic band diagram of the porous SiC film of the sample SiC-60 at low temperature was shown in Fig. 11. In the PL of oxygen vacancy of silica, the rest energy of excitation photon (325 nm, 3.82 eV) can be converted into phonons. The phonons participating in PL of 6H-SiC (3.34 eV) and 3C-SiC (2.305 eV) may be supplied by the phonon scattering between the interface of SiC and silica.

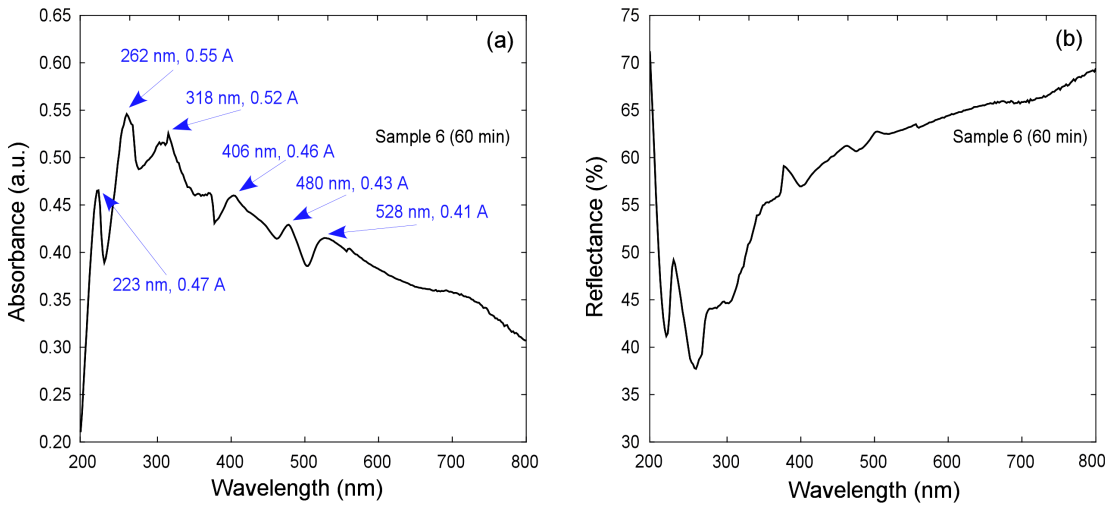

Figure 10. Ultraviolet-visible spectrum of the porous SiC film deposited for 60 min: a) absorbance and b) reflectance spectra (A represents absorbance)

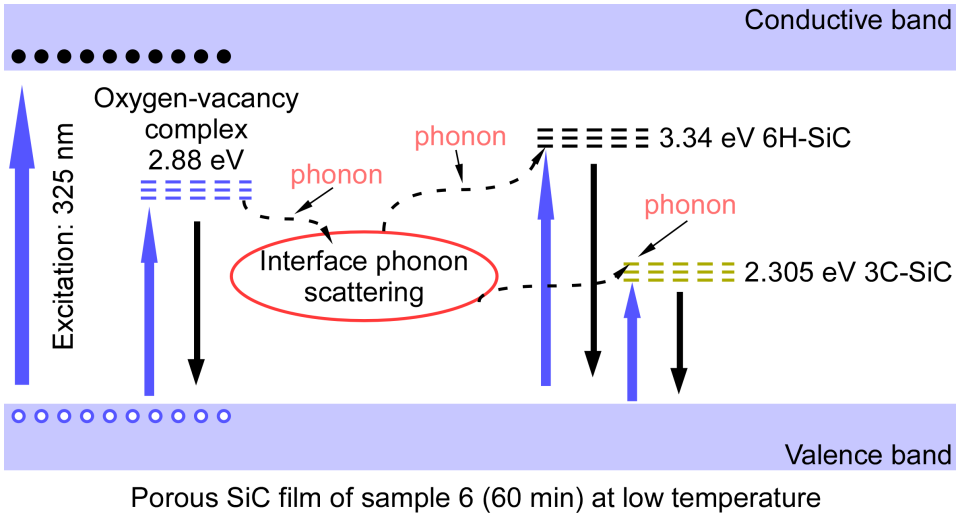

Figure 11. The schematic band diagram of the porous SiC film of the sample SiC-60 at low temperature

IV. Conclusions

In conclusion, we obtained the porous fluorescent SiC films by using porous AAO template assisted magnetron sputtering processing. The SiC film deposited for 60 min showed macroporous structure with the pore size of 200 to 250 nm and pore spacing of 450 nm. The PL spectrum of the porous SiC film ranged from 400 to 700 nm. The band gap of the porous SiC film was 2.305 eV, and the phonon energy of phonon participating in PL of SiC is simulated at 0.075 eV. The band gap of oxygen defect of silica in SiC is estimated at 2.88 eV. The phonons participating in PL of SiC may be from phonon scattering between the interface of SiC and silica. There are potential applications of porous fluorescent SiC in white LED and photoelectric sensor detectors.

Acknowledgements: The authors would like to acknowledge Dr. Hong Cheng of Huazhong University of Science & Technology Analytical & Testing Center for the fluorescence spectrum testing. This research was supported by National Innovation and Entrepreneurship Training Program for College Students (No. 201910497132), the National Natural Science Foundation of China (No. 11747133), and the Fundamental Research Funds for the Central Universities (No. 195209019). We acknowledge Dr. Tingting Luo (the Nanostructure Research Center (NRC), the center for materials research and analysis of Wuhan University of Technology) for the help in S/TEM analysis.

References

1. M. Bhatnagar, B.J. Baliga, "Comparison of 6H-SiC, 3C-SiC, and Si for power devices", *IEEE T. Electron Dev.*, **40** [3] (1993) 645–655.
2. R. Madar, "Silicon carbide in contention", *Nature*, **430** [7003] (2004) 974–975.
3. C.R. Eddy, D.K. Gaskill, "Silicon carbide as a platform for power electronics", *Science*, **324** [5933] (2009) 1398–1400.
4. F. Roccaforte, P. Fiorenza, G. Greco, R. Nigro, F. Giannazzo, F. Lucolano, M. Saggio, "Emerging trends in wide band gap semiconductors (SiC and GaN) technology for power devices", *Microelectronic Eng.*, **187-188** [2] (2018) 66–77.
5. K. Kornaus, G. Grabowski, M. Raczka, D. Zientara, A. Gubernat, "Mechanical properties of hot-pressed SiC-TiC composites", *Process. Appl. Ceram.*, **11** [4] (2017) 329–336.
6. H. Morkoc, S.S. Strite, G.B. Gao, M.E. Lin, B. Sverdlov, M. Burns, "Large-band-gap SiC, III-V nitride, and II-VI ZnSe-based semiconductor device technologies", *J. Appl. Phys.*, **76** [3] (1994) 1363–1398.
7. Y.X. Wang, H.P. He, H.G. Tang, "Progress in research on wide band-gap semiconductor SiC and its application", *J. Chin. Ceram. Soc.*, **30** [3] (2002) 372–381.
8. T. Matsumoto, J. Takahashi, T. Tamaki, T. Futagi, H. Mimura, "Blue-green luminescence from porous silicon carbide ", *Appl. Phys. Lett.*, **64** [2] (1994) 226.
9. V. Petrova-Koch, O. Sreseli, G. Polisski, D. Kovalev, T. Muschik, F. Koch, "Luminescence enhancement by electrochemical etching of SiC(6H)", *Thin Solid Films*, **255** [1-2] (1995) 107–110.
10. W. Lu, Y. Ou, E.M. Fiordaliso, Y. Iwasa, V. Jokubavicius, M. Syvajarvi, S. Kamiyama, P. Petesen, H. Ou, "White light emission from fluorescent SiC with porous surface", *Sci. Rep.*, **7** [1] (2017) 9798.
11. W. Lu, A.T. Tarekegne, Y. Ou, S. Kamiyama, H. Ou, "Temperature-dependent photoluminescence properties of porous fuorescent SiC", *Sci. Rep.*, **9** [1] (2019) 16333.
12. Z. Li, L. Yang, D. Ge, Y. Ding, L. Pan, J. Zhao, Y. Li, "Magnetron sputtering SiC films on nickel photonic crystals with high emissivity for high temperature applications", *Appl. Surf. Sci.*, **259** (2012) 811–815.
13. Z. Li, D. Ge, L. Yang, X. Liu, Y. Ding, L. Pan, J. Zhao, Y. Li, "Facile synthesis and improved photoluminescence of periodic SiC nanorod arrays by SiO_2 templates-assisted magnetron sputtering method", *J. Alloy. Compd.*, **537** (2012) 50–53.
14. P.J. Kelly, R.D. Arnell, "Magnetron sputtering: a review of recent developments and applications", *Vacuum*, **56** (2000) 159–172.
15. J. Wasyluk, T.S. Perova, S.A. Kukushkin, A.V. Osipov,

N.A. Feoktistov, S.A. Grudinkin, "Raman investigation of different polytypes in SiC thin films grown by solid-gas phase epitaxy on Si (111) and 6H-SiC substrates", *Mater. Sci. Forum*, **645-648** (2010) 359–362.

16. Z. Li, J. Zhao, M. Zhang, J. Xia, A. Meng, "SiC nanowires with thickness-controlled SiO_2 shells: Fabrication, mechanism, reaction kinetics and photoluminescence properties", *Nano Res.*, **7** (2014) 462–472.
17. W. Lu, I. Wasa, Y. Ou, D. Jinno, S. Kamiyama, P.M. Petersen, H. Ou, "Effective optimization of surface passivation on porous silicon carbide using atomic layer deposited Al_2O_3", *RSC Adv.*, **7** (2017) 8090–8097.